Modulation of the ligational properties of a new cylindrical macrotricycle by coupling of photochemical- and pH-switching properties

Andrea Bencini,[a] M. Alexandra Bernardo,[b] Antonio Bianchi,*[,a] Mario Ciampolini,*[,a] Vieri Fusi,[c] Nicoletta Nardi,[a] A. Jorge Parola,[b] Fernando Pina*[,b] and Barbara Valtancoli[a]

[a] *Department of Chemistry, University of Florence, via Maragliano 75/77, 50144 Florence, Italy*
[b] *Departamento de Química, Universidade Nova de Lisboa, Quinta da Torre, 2825 Monte da Caparica, Lisboa, Portugal*
[c] *Institute of Chemical Sciences, University of Urbino, Piazza Rinascimento 6, 61026 Urbino, Italy*

The new cylindrical molecule L containing two tetraazamacrocyclic rings linked by two azobenzene pillars displays photoelastic properties. Light absorption at 366 nm gives rise to *trans* ⟶ *cis* isomerization of the azobenzene moieties producing two isomers containing one or two *cis*-azobenzenes, respectively. The three *trans-trans* (*E-E*), *trans-cis* (*E-Z*) and *cis-cis* (*Z-Z*) isomers have been identified and characterized by ^{1}H NMR spectroscopy, allowing the dependence of their formation percentages with irradiation time to be determined. The sequence of photochemical reactions *E-E* ⟶ *E-Z* ⟶ *Z-Z* allows almost complete conversion of the *E-E* into the *Z-Z* isomer at 366 nm and 298 K. Both thermal ($k = 1.75 \times 10^{-5}$ s^{-1} at 313 K) and photo-induced (at 436 and 313 nm) back-isomerization reactions have been studied. The protonation constants of the three isomers in equimolar solutions of water–DMSO indicate a decreasing basicity in the order *E-E* > *E-Z* > *Z-Z*, in agreement with increasing electrostatic repulsion between the positive charges caused by a reduction in the separation between the protonation sites occurring upon *Z* ⟶ *E* isomerization.

Photoisomerization of azobenzene units has been used to switch several properties in large molecules and supramolecular systems.[1,2] One example involves the crown ethers with an intermolecular bridge containing this unit, which become photo-responsive towards different ions.[1–3] Other examples are: macrocyclic and macrobicyclic species whose cavity size can be controlled by light;[4] azobenzene-capped β-cyclodextrins (CD) in which *trans* ⟶ *cis* photoisomerization of the cap-azobenzene can expand the CD cavity, so changing the binding ability of the receptor towards several substrates;[5,6] and cylindrical structures obtained by linking two macrocycles by two or more pillars containing azobenzenes,[7,8] displaying 'photoelastic' properties. Cyclophane-like crown ethers,[9] and 'butterfly' azobis(crown ethers)[10–12] whose *trans* ⟶ *cis* (*E-Z*) isomerization resembles the motion of a butterfly, also change their ion selectivity upon irradiation.

Ligand selectivity towards metal cation and, more recently, anion coordination has been extensively achieved by proton-mediated switching (pH-switching), taking advantage of the protonation equilibria involving most of the ligands in solution. From this point of view polyazamacrocycles have proved particularly useful owing to the convergent array of binding groups within their molecular structures.[13–15]

Shinkai *et al.* synthesized and studied a cylindrical molecule containing two 1,10-diaza-4,7,13,16-tetraoxacyclooctadecane rings connected *via* amidic linkages to azobenzene pillars, evidencing the photoresponsive character of its ligational properties.[8] This work suggested to us the possible synthesis of a new macrotricyclic cylindrical ligand (**L**), composed of two azobenzene pillars and two tetraazamacrocyclic rings, which combines photoelastic characteristics and pH-mediated binding properties. As shown by the photochemical and thermodynamic studies presented below, combination of these two switching mechanisms leads to the modulation of the ligational properties of this molecule in both the cavity size and the availability of binding sites.

Results and discussion

Synthesis

Shinkai *et al.* confirmed that when the dimensions of the reacting fragments do not fit each other, as in the equimolar reaction of 1,10-diaza-4,7,13,16-tetraoxacyclooctadecane with 4,4′-bis-(chloroformyl)azobenzene, the 2:2 adduct results in a satisfactory yield (21%) when using a high dilution method.[8] An analogous 2:2 condensation (Scheme 1) was employed in the preparation of the new molecule **L**. In this case the greater difference between the reactants' length favours such reaction stoichiometry, affording **L** in good yield (34%), even though a high dilution method was not used.

Characterisation of *E-E*, *E-Z* and *Z-Z* isomers by NMR spectroscopy

The *E-E*, *E-Z*, and *Z-Z* forms of **L** can be identified and quantified by NMR spectroscopy in solution.

Solutions of **L** in $CDCl_3$ present the ^{1}H NMR spectrum reported in Fig. 1(*a*), which can be ascribed to a single form of the molecule (*E-E*). Irradiation of such samples at 366 nm gives rise to new signals whose relative intensities vary with irradiation time, accounting for the formation of another two forms of **L**. Fig. 1(*b*) and 1(*c*) show the ^{1}H NMR spectra of **L** recorded after 20 and 55 min, respectively, representing two different stages in the photo-isomerization corresponding to the coexistence of the three isomers [Fig. 1(*b*)] and to the almost complete conversion of the *E-E* form into the *E-Z* and *Z-Z* isomers [Fig. 1(*c*)].

From ^{1}H-^{1}H and ^{1}H-^{13}C two-dimensional correlation experiments the signals in these spectra can be unambiguously assigned.

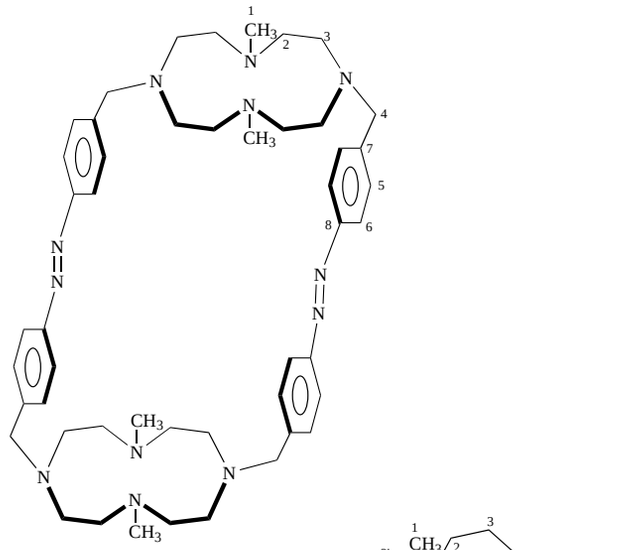

L, *E-E*

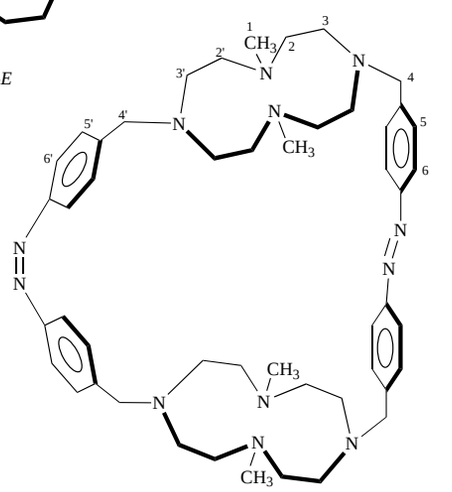

E-Z

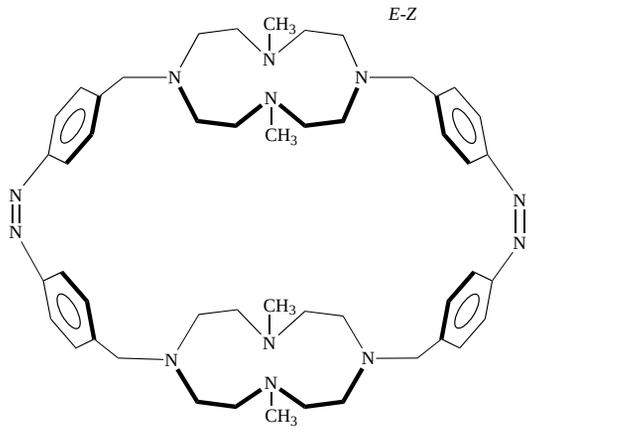

Z-Z

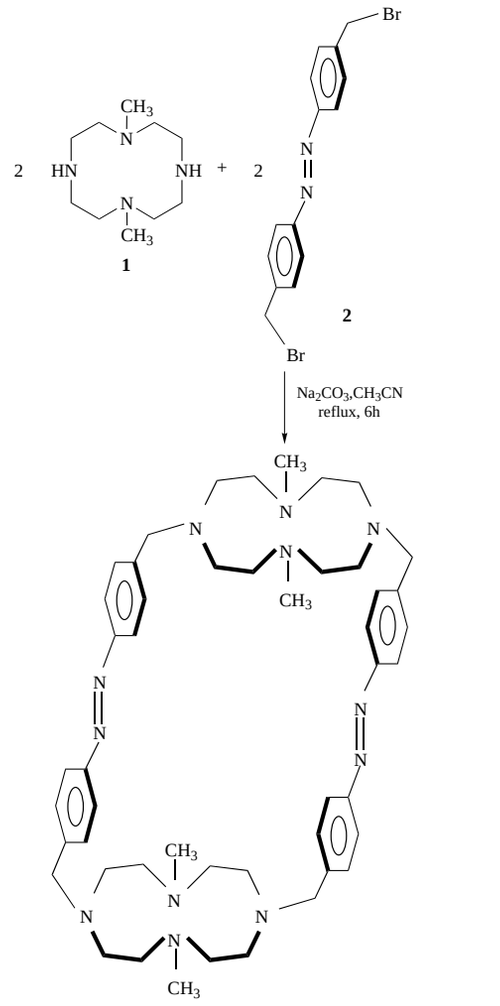

L

Scheme 1

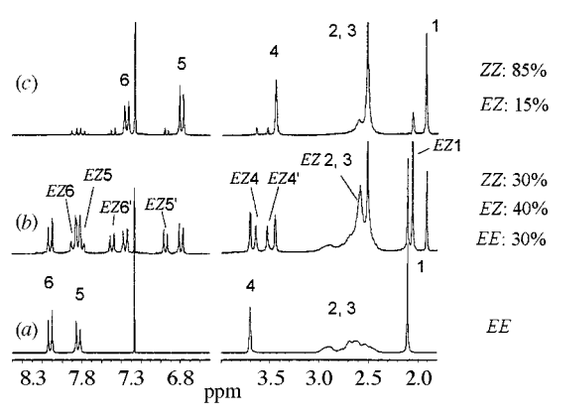

Fig. 1 ^{1}H NMR spectra of the *E-E*, *E-Z* and *Z-Z* isomers of **L** in $CDCl_3$. For labelling, see ligand drawing.

The spectrum of the *E-E* form [Fig. 1(*a*)] shows a singlet (1) at 2.02 ppm integrating 12 H (the methylic protons), a broad band (2, 3) at 2.30–2.85 ppm integrating 32 H (the protons of the ethylenic chains), a singlet (4) at 3.63 ppm integrating 8 H (the benzylic protons), and the signals of an AA′BB′ system (5, 6) at 7.76 and 8.04 (the aromatic protons), each integrating 8 H. These spectral features are indicative of D_{2h} symmetry, averaged on the NMR time scale.

Integration of the signals in the ^{1}H NMR spectrum reported in Fig. 1(*c*) allows a determination of the relative abundance of the *E-Z* and *Z-Z* forms of 15% and 85%, respectively. As far as the *Z-Z* form is considered, its ^{1}H NMR spectrum consists of a singlet (1) at 1.83 ppm (12 H, the methylic protons), a broad band (2, 3) at 2.40–2.63 ppm (32 H, the protons of the ethylenic chains), a singlet (4) at 3.37 ppm (8 H, the benzylic protons), and the signals of a AA′BB′ system (5, 6) at 6.72 and 7.28 (8 H each one, aromatic protons). These characteristics confirm that **L** presents in its *Z-Z* form the same D_{2h} time-averaged symmetry observed for the *E-E* isomer.

Excluding the ^{1}H NMR signals corresponding to the *E-E* and *Z-Z* forms, we can easily identify the peaks corresponding to the intermediate *E-Z* isomer in the spectra reported in Fig. 1(*b*) and 1(*c*). The spectrum is composed of a singlet at 1.97 ppm (12 H, the methylic protons), a broad band at 2.35–2.75 ppm (32 H, the protons of the ethylenic chains), two singlets at 3.45 and 3.57 ppm (4 H each one, the benzylic protons), and the signals of two AA′BB′ systems at 6.86, 7.42, 7.72 and 7.80 ppm (4 H

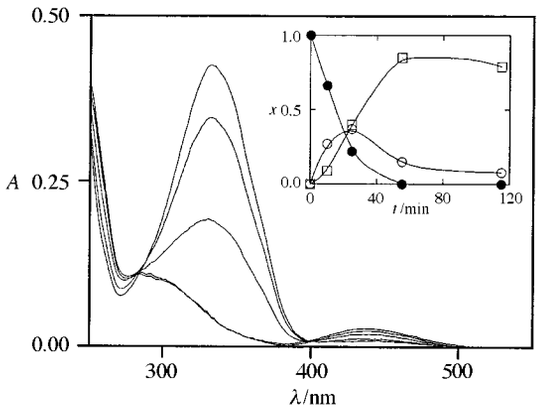

Fig. 2 Spectral variations of **L** in $CDCl_3$ (1×10^{-5} mol dm^{-3}) upon irradiation at 366 nm; irradiation time: 0; 10; 25; 55; 115 min. Inset: molar fraction distribution of the three species calculated from the ^1H NMR data in Table 1, for the same irradiation times: ●, *E-E*; ○, *E-Z*; □, *Z-Z*.

Table 1 Molar fractions of the *E-E*, *E-Z*, and *Z-Z* isomers of **L** present in chloroform solution as a function of irradiation time at 366 nm

	Molar fractions		
Time/min	*E-E*	*E-Z*	*Z-Z*
0	1	0	0
10	0.66	0.27	0.09
25	0.22	0.37	0.40
55	0	0.15	0.85
115	0	0.08	0.79

each one, aromatic protons) in accordance with C_{2v} symmetry, averaged on the NMR time scale. Integration of the signals in the spectrum shown in Fig. 1(*b*) yields the relative percentages of the three isomers in the corresponding sample (*E-E* 30%, *E-Z* 40%, *Z-Z* 30%).

It is interesting to note that in $CDCl_3$ solution **L** presents the highest symmetry consistent with each of the three different isomers. In the *E-Z* isomer the lower symmetry of the molecule (C_{2v}) observed on the NMR time scale with respect to the *E-E* and *Z-Z* forms (D_{2h}) derives from the absence in the former isomer of a symmetry plane passing through the methylated nitrogens and the methyl groups.

E-E ⟶ *Z-Z* photoisomerization

The absorption spectrum of the *E-E* form of **L** in $CHCl_3$ (Fig. 2) is quite similar to the parent compound *E*-azobenzene.[1] The first singlet shows a low intensity band (930 $м^{-1}$ cm^{-1}) centred at 436 nm, immediately recognized as the $^1(n,\pi^*)$ state, while the high intensity band, (42 600 $м^{-1}$ cm^{-1}), with a maximum at 332 nm, can be attributed to the $^1(\pi,\pi^*)$ state. As in azobenzene the two singlets are separated by a large energy gap.

As previously observed, light absorption by the *E-E* isomer of **L** in chloroform gives rise to isomerization of the molecule producing the *Z-Z* form *via* the intermediate *E-Z* species. This important result prompted us to carry out a more systematic study of the photochemical processes involving this compound.

A solution of the *E-E* form (2×10^{-3} mol dm^{-3}) in $CDCl_3$ was irradiated at 366 nm and the photochemical reaction was followed simultaneously by ^1H NMR and UV-VIS absorption spectrophotometry as a function of the irradiation time. The pattern observed (Fig. 2) is quite similar to that reported for azobenzene itself and for some of its derivatives.[2–12] As reported in the previous section, the three isomers can be clearly identified and quantified, in solution, by NMR spectroscopy; the molar fractions of each isomer after irradiation of 10, 25, 55, and 115 min are reported in Table 1 and depicted in the inset of Fig. 2.

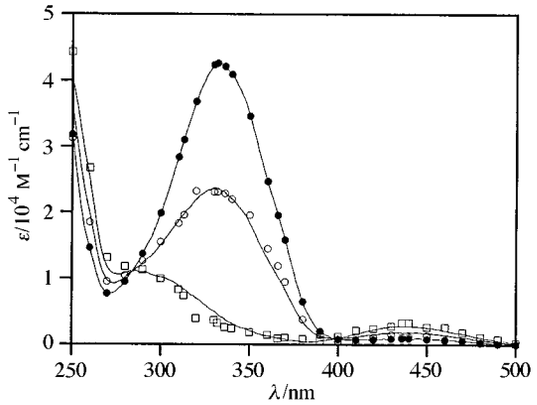

Fig. 3 Absorption spectra of three **L** isomers in $CHCl_3$: ●, *E-E*; ○, *E-Z*; □, *Z-Z*

This inset clearly confirms that the kinetic process in the photochemical reaction consists of two consecutive reactions according to a scheme (*E-E* ⟶ *E-Z* ⟶ *Z-Z*) in which formation of the *Z-Z* isomer occurs from the intermediate *E-Z* form. Conversion to the *Z-Z* isomer is almost (but not totally) complete, and is accompanied by a less efficient photochemical degradation of the compound.

The simultaneous use of the data obtained from ^1H NMR and UV-VIS absorption spectrophotometry allows us to calculate (Appendix 1) the molar absorption coefficients of the three isomers, furnishing the spectrum of each form (Fig. 3). These spectra account for the almost complete conversion of the compound into the *Z-Z* form by irradiation at 366 nm, since at this wavelength only the *E-E* and *E-Z* forms, but not the *Z-Z*, offer efficient light absorption.

The most interesting feature in Fig. 3 is the fact that the absorption spectrum of the *E-Z* form is composed of exactly half the spectrum of the *E-E* form and half the spectrum of the *Z-Z* form, as expected for two independent chromophore groups. This result indicates that by exclusive use of UV-VIS absorption data alone, it is not possible to determine the molar fraction distribution of the three species; only the total amount of the *E* and *Z* forms of azobenzene groups, independent of their belonging to a particular isomer, can be obtained.

The absorption spectrum of the *Z-Z* form in $CHCl_3$ is identical to that of *Z*-azobenzene,[1] showing a first singlet $^1(n \longrightarrow \pi^*)$ at 436 nm (2800 $м^{-1}$ cm^{-1}) and a second singlet $^1(\pi \longrightarrow \pi^*)$ at 286 nm (11 200 $м^{-1}$ cm^{-1}). According to these data, the chromophore azobenzene can be considered as being chiefly responsible for the characteristics of the absorption spectrum of **L**.

We carried out additional analogous photoisomerization reactions in other solvents including acidic water, acidic chloroform and DMSO–H_2O mixture. The results obtained confirm that the photochemical behaviour of **L** in these solvents is qualitatively similar to the behaviour observed in chloroform, while differences are found in the dependence of isomerization yields on irradiation time.

In all the solvent systems studied we detected no fluorescence emission at room temperature for the three isomers.

Z-Z ⟶ *E-E* photoisomerization

In order to study the inverse photochemical reaction *Z* ⟶ *E*, a $CHCl_3$ solution containing more than 90% of the *Z-Z* form was prepared by irradiation at 366 nm. Two different portions of this solution were then subjected to a second irradiation, one at 436 nm and the other at 313 nm, and back-isomerization was observed as shown in Fig. 4.

As observed in Fig. 4, the photochemical reaction is reversible back to the *E-E* form. However, the back reaction is more efficient at 436 nm than at 313 nm. The reasons for this behaviour are related to the amount of incident light absorbed

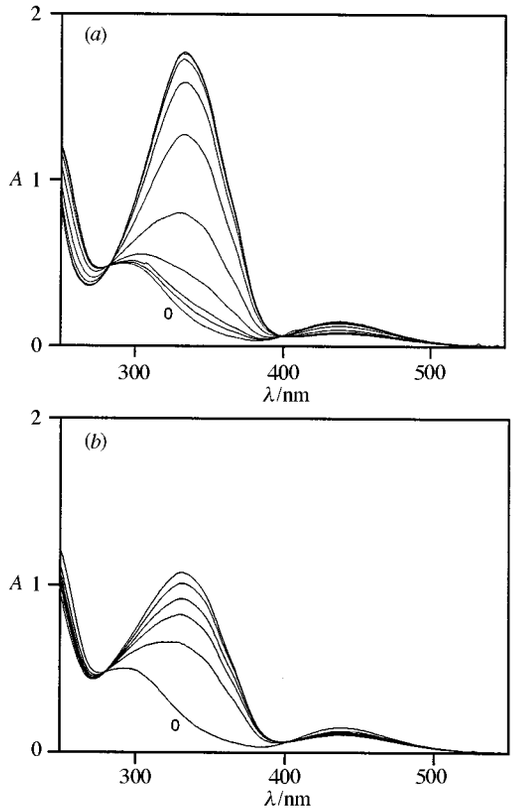

Fig. 4 Spectral variations of **L** (5×10^{-5} mol dm^{-3}, $CHCl_3$) upon irradiation of a mixture containing more than 90% of the *Z-Z* isomer at 436 nm (*a*) and at 313 nm (*b*) at increasing irradiation times: respectively, (*a*) 0, 0.5, 1, 3, 9, 19, 34, 54, 84 and 144 min; (*b*) 0, 0.5, 1, 1.5, 2.5 and 4.5 min. The same equilibrium spectra are obtained if the starting compound is the *E-E* isomer.

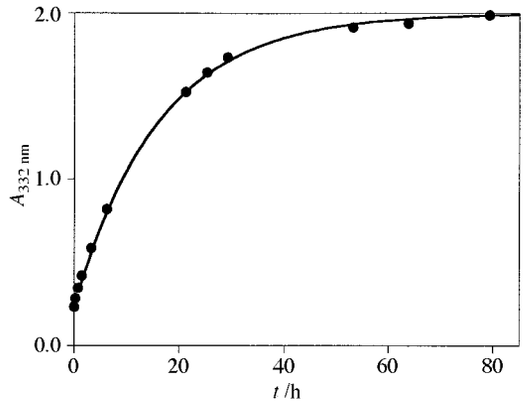

Fig. 5 Thermal recovery of the *E-E* isomer from the *Z-Z* isomer in $CHCl_3$ at 313 K followed by the time dependence of the peak absorbance at 332 nm in the spectrum of the *E-E* isomer

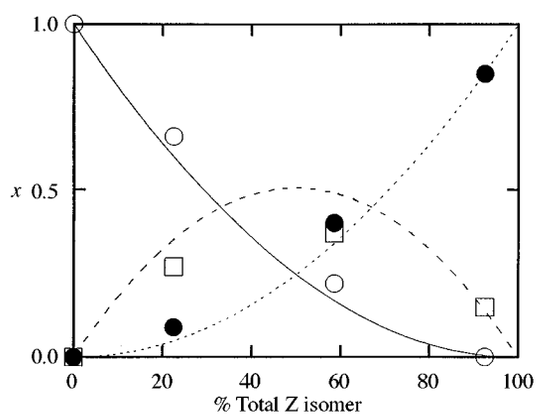

Fig. 6 Molar fraction distribution of the three **L** isomers as a function of total *Z* (*cis*) conformations. Symbols ○ (*E-E*), □ (*E-Z*) and ● (*Z-Z*) represent experimental data (Table 1); lines correspond to the values obtained by statistical treatment.

by each species. In the previous section we remarked that at 366 nm almost total conversion into the *Z-Z* form is possible, due to the very small molar absorption coefficient of this species relative to the other (Fig. 2). In contrast, the *Z-Z* form is the highest absorbing species at 436 nm and photochemical conversion to the *E-E* isomer can occur efficiently at this wavelength [Fig. 4(*a*)]. An intermediate situation is observed at 313 nm. In this case absorption of the *Z-Z* isomer is more favourable than at 366 nm, but less so than at 436 nm, and the back photoisomerization reaction *Z-Z* ⟶ *E-E* occurs only partially [Fig. 4(*b*)].

Thermal recovery of the *E-E* form

As with the other azobenzene compounds the most stable form of **L** is the *E-E* isomer, and for this reason back recovery of the *E-E* species is obtained thermally from the *Z-Z* species. However, this reaction is very slow at room temperature, and for this reason we followed the thermal reisomerization reaction at 313 K. The absorbance increase at the maximum absorption wavelength (332 nm) of the *E-E* form, at this temperature, is shown in Fig. 5. The time dependence of the absorption data represented in Fig. 5 satisfies a first-order rate equation with rate constant $k = 1.75 \times 10^{-5}$ s^{-1} (lifetime of 15.9 h).

This result seems to indicate that the two *Z* ⟶ *E* thermal isomerizations in each molecule are independent, as observed in the photochemical reactions, and hence these kinetic data account for the conversion of total *Z* forms to total *E* forms independent of the different isomers. In order to verify the independence of these isomerization events, a quantitative statistic treatment was carried out to fit the molar fraction distribution of the three isomers deduced by ^{1}H NMR data. The results obtained by the statistical method (Appendix 2) are depicted in Fig. 6, the lines representing the theoretical curves and the symbols the experimental molar fractions (Table 1). Taking into consideration the uncertainties in measuring the areas of ^{1}H NMR peaks, Fig. 6 shows good agreement between calculated and experimental data, confirming the independence of the photoisomerization events.

Table 2 Quantum yields (Φ) for the photoisomerization of **L** in chloroform, acidic chloroform and acidic aqueous solutions

	$CHCl_3$		$CHCl_3/H^+$		H_2O/H^+	
	365 nm	436 nm	365 nm	436 nm	365 nm	436 nm
$\Phi_{E\text{-}E \longrightarrow E\text{-}Z}$	0.09	—	0.04	—	0.05	—
$\Phi_{Z\text{-}Z \longrightarrow E\text{-}Z}$	—	0.09	—	0.08	—	0.07

Quantum yields

Measurements of the quantum yields for the processes involved in this system present some experimental limitations. In effect, while it is possible to calculate the quantum yield of the photoreactions *E-E* ⟶ *E-Z* and *Z-Z* ⟶ *E-Z*, starting from solutions containing almost only the *E-E* or the *Z-Z* species, this is not possible for the photoreactions of the *E-Z* species since solutions containing only this species are not available.

Table 2 reports the quantum yields (Φ) for the photoisomerizations of **L** in chloroform, acidic chloroform and acidic water.

Comparison of these quantum yields with those of azobenzene in *n*-hexane, $\Phi_{E \longrightarrow Z} = 0.10$ and 0.25, respectively at 313 and 436 nm, and $\Phi_{Z \longrightarrow E} = 0.44$ and 0.51, respectively at 313 and 436 nm,[16] shows that isomerization of **L** is less efficient in

Table 3 Logarithms of the protonation constants of the *E-E*, *E-Z* and *Z-Z* isomers of **L** determined in equimolar DMSO–H_2O mixture, 0.1 mol dm^{-3} Me_4NNO_3, at 298.1 ± 0.1 K

Reaction	log *K*		
	E-E	*E-Z*	*Z-Z*
$H_2L^{2+} + H^+ \rightleftharpoons H_3L^{3+}$	4.74(3)	4.36(8)	4.07(7)
$H_3L^{3+} + H^+ \rightleftharpoons H_4L^{4+}$	3.53(3)	3.21(8)	2.93(7)

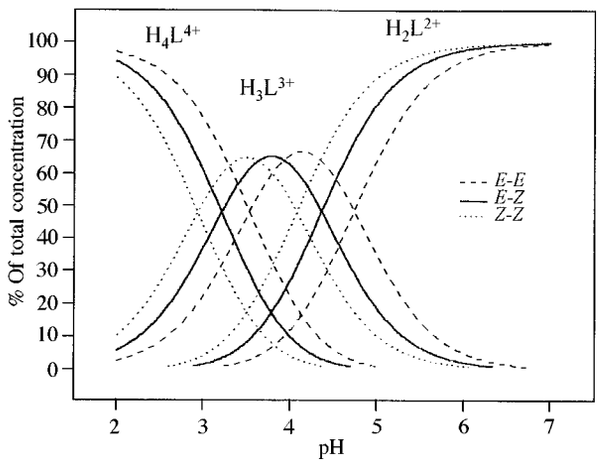

Fig. 7 Superimposed distribution diagrams of the protonated species formed by the three **L** isomers as a function of pH ([**L**] = 1 × 10^{-3} mol dm^{-3}, DMSO–H_2O 50 : 50 mol : mol, 298.1 K)

both directions, in agreement with the expected greater rigidity of the macrotricyclic molecule.

The quantum yield *Z-Z* ⟶ *E-E* is slightly higher than *E-E* ⟶ *Z-Z*, as in the case of azobenzene, except for neutral chloroform where we detected no difference within experimental errors.

Another interesting feature is the lower quantum yield for the *E-E* ⟶ *Z-Z* isomerization in acidic media compared with neutral solutions. In order to gain an insight into this aspect, we have analysed the basicity properties of the different isomers.

Photomodulation of basicity properties

Compound **L** is appreciably soluble in water only at very acidic pH values; for this reason we used an equimolar DMSO–H_2O mixture as a solvent for the determination of the protonation constants of the three **L** isomers, according to the procedure reported in the experimental section. Also, in this solvent mixture the solubility of the compound is restricted to a rather narrow pH range (pH < 6.4 for [**L**] = 8 × 10^{-4} mol dm^{-3} at 298.1 K in 0.1 mol dm^{-3} Me_4NNO_3) in which only the species $H_2\mathbf{L}^{2+}$, $H_3\mathbf{L}^{3+}$ and $H_4\mathbf{L}^{4+}$ were detected. Hence, under these conditions, it was possible to determine only the equilibrium constants associated with the protonation reactions of $H_2\mathbf{L}^{2+}$ and $H_3\mathbf{L}^{3+}$ (Table 3). Although the basicity behaviour of **L** is not completely defined, these protonation constants provide useful information on the modifications brought about by light absorption on the proton transfer properties of such molecules. As can be seen from Table 3, the basicity of the three isomers decreases in the order *E-E* > *E-Z* > *Z-Z*. The conversion of the azobenzene groups from *E* to *Z* conformation causes a reduction in the separation between the two tetraazamacrocyclic moieties—the locations of the H^+ ions in the protonated forms of **L**—increasing the electrostatic repulsion between positive charges. The increased electrostatic repulsion can explain the reduced basicity of the molecules in the successive protonation steps according to the observed trend (*E-E* > *E-Z* > *Z-Z*). As a consequence **L** undergoes protonation at different pH values, depending on the particular isomer, as evidenced by the superimposed distribution diagrams of the protonated species formed by each isomer as a function of pH (Fig. 7).

This result offers a justification of the lower quantum yield observed in the photoinduced *E-E* ⟶ *Z-Z* isomerization reactions in acidic media compared with neutral solutions (Table 2). While in neutral chloroform **L** is present in its unprotonated form, the principal species in the acidic solutions should be the tetracharged $H_4\mathbf{L}^{4+}$ cation, which is expected to resist much more than **L** such molecular reorganization due to the stiffness produced by the electrostatic repulsion between the ammonium groups. Indeed, the lowest quantum yields are observed for the *E-E* ⟶ *Z-Z* isomerization reactions which cause a shortening of the separation between the positive charges in the protonated molecule.

Conclusions

The structural effect of light absorption by **L** involves a conformational change from a cylindrical towards a more circular structure, taking place *via* two independent photoisomerization reactions *E-E* ⟶ *E-Z* ⟶ *Z-Z*. The *Z* form of the azobenzene groups are readily obtained by irradiation at 366 nm and recovery of the more stable *E* form can be achieved by thermal reisomerization or, more efficiently, by irradiation at 436 nm. Similar behaviour was previously observed by Shinkai *et al.* for another photoresponsive cylindrical molecule, but in that case accumulation of *E-Z* intermediate along the isomerization pathway was not found. In our case, light absorption by **L** produces a more gradual ligand modification which is accompanied by progressive alteration of the ligand basicity properties. Namely, different physico-chemical properties of **L** can be switched on and off, and modulated, by light irradiation at distinct wavelengths.

Protonation of polyamines controls the ability of such molecules to associate with chemical species, competing with the formation of metal complexes and promoting anion binding. In this sense, protonation itself is a sort of chemical switch. The results presented here confirm that coupling of photochemical- and pH-switching characteristics makes possible a modulation of the ligational properties of **L**, producing a number of diverse species differing in the conformation of the binding cavity and/or the nature of the binding sites. For instance, as far as the binding of anionic species is concerned, the protonated forms of **L** could be relevant in molecular recognition processes, based on pH-dependent size and/or geometric criteria, which can be controlled 'from outside' by light.

Further work will be undertaken to gain an insight into the switching of such coordination reactions.

Experimental

Synthesis

All reagents and solvents were purchased from commercial sources and used as received unless otherwise noted. 1,7-Dimethyl-1,4,7,10-tetraazacyclododecane **1**[17] was synthesized as previously reported.

Compound L. This compound was synthesized by following the procedure depicted in Scheme 1. A solution of **1** (0.54 g, 2.7 mmol), **2** (1.0 g, 2.7 mmol) in the presence of Na_2CO_3 (0.60 g, 5.5 mmol) in dry CH_3CN was refluxed for 6 h. The mixture was then cooled at room temperature, filtered and the resulting solution was evaporated to dryness on a rotary evaporator. The crude product was dissolved in chloroform and chromatographed over a Al_2O_3 column using chloroform–methanol (97 : 3). The red fraction of the eluted solution was evaporated to dryness leaving an orange residue which was recrystallized from hot CH_3CN (0.38 g, 34%), mp > 300 °C. (Found: C, 71.0; H, 8.5; N, 20.2. Calc. for $C_{48}H_{68}N_{12}$: C, 70.9; H, 8.4; N, 20.7%). NMR ($CDCl_3$) ^{13}C; 44.0, 53.9, 56.8, 60.0, 122.9, 129.9, 144.8, 151.7. The compound could be recrystallized from hot benzene.

NMR measurements

^{1}H and ^{13}C NMR spectra were recorded in D_2O at 298 K on a Bruker AC-200 spectrometer operating at 200 MHz for ^{1}H and 50.32 for ^{13}C. ^{1}H NMR peak positions are reported relative to HOD at 4.75 ppm, while dioxane ($\delta = 67.4$) was used as a reference standard for ^{13}C spectra. ^{1}H and ^{13}C NMR spectra in $CDCl_3$ were obtained at 298 K using TMS as a reference standard.

Spectrophotometric measurements

Electronic spectra were recorded on a Perkin-Elmer Lambda 9 spectrophotometer equipped with a 1 cm cell thermostatted at 298 K.

Irradiation experiments

Light excitation was performed by a medium pressure mercury arc lamp. Interference filters (Oriel) were used to select narrow spectral ranges with maximum wavelengths at 313, 366 and 436 nm. The irradiated solution was contained in a 1 cm spectrophotometric quartz cell. The intensity of the incident light (7.6×10^{-7} Einstein min^{-1} at 313 nm, 1.1×10^{-6} Einstein min^{-1} at 366 nm, 3.2×10^{-7} Einstein min^{-1} at 436 nm) was measured by ferrioxalate actinometry.[18]

Potentiometric measurements

Potentiometric (pH-metric) measurements ($pH = -\log [H^+]$) were carried out in a degassed equimolar H_2O–DMSO mixture, 0.1 mol dm^{-3} Me_4NNO_3, at 298.1 ± 0.1 K, using the equipment and the methodology that has been already described for aqueous solutions.[19] The combined Ingold 405 S7/120 electrode was calibrated as a hydrogen concentration probe by titrating known amounts of HCl with CO_2-free Me_4NOH solutions and determining the equivalent point by Gran's method[20] which allows us to determine the standard potential E° and the ionic product of water [$pK_w = 18.12(1)$ at 298.1 K in 0.1 mol dm^{-3} Me_4NNO_3]. All measurements were performed in the pH range 2.4–6.4; at high pH values precipitation was observed. An empirical correction was applied for the liquid junction potential in very acidic solutions. In all experiments the concentration of **L** was *ca.* 8×10^{-4} mol dm^{-3}. Three measurements (*ca.* 120 data points) were performed to determine the protonation constants of **L** in its stable *E-E* form, processing of the emf data being performed with the computer program HYPERQUAD.[21] Solutions containing known amounts of the *E-E*, *E-Z* and *Z-Z* isomers were prepared by irradiation at 366 nm of standardized solutions of the *E-E* form and used to perform potentiometric titrations at 298.1 ± 0.1 K in the dark. The concentration of each isomer was determined by means of ^{1}H NMR spectroscopy, following the same criterion previously described for chloroform solutions. ^{1}H NMR measurements were also employed to demonstrate that under our experimental conditions (darkness, 298 K), no appreciable changes in the concentration of the three isomers, due to thermal re-equilibration and/or to change of solution pH, occur during the time required for potentiometric titration (*ca.* 2 h). Three measurements were performed employing solutions with different percentages of the three isomers. The computer program HYPERQUAD[21] was used to calculate the protonation constants of the *E-Z* and *Z-Z* isomers from emf data. The protonation constants of the *E-E* isomer were kept constant during calculations.

Appendix 1

Calculation of the molar absorption coefficients of the three species

At each irradiation time one aliquot of 15 μl was extracted and diluted to 3 ml with $CHCl_3$ in order to obtain the respective absorption spectrum reported in Fig. 2. Calculation of the three molar absorption coefficients was carried out by resolving eqns. (i)–(iii), where C_0 is the total concentration, ε_a, ε_b, ε_c are the molar absorption coefficients, respectively, of the species *E-E*, *E-Z* and *Z-Z*, and the coefficients that multiply the molar absorption coefficients are obtained according to the data in Table 1. The solution of this system gives the molar absorption coefficients of the three species at each wavelength. The results of this procedure are shown in Fig. 6.

$$\varepsilon_{a(\lambda)} = A_\lambda(0 \text{ min})/C_0 \quad \text{(i)}$$

$$A_\lambda(10 \text{ min}) = [0.66\varepsilon_{a(\lambda)} + 0.27\varepsilon_{b(\lambda)} + 0.09\varepsilon_{c(\lambda)}]C_0 \quad \text{(ii)}$$

$$A_\lambda(25 \text{ min}) = [0.22\varepsilon_{a(\lambda)} + 0.37\varepsilon_{b(\lambda)} + 0.40\varepsilon_{c(\lambda)}]C_0 \quad \text{(iii)}$$

Appendix 2

Statistical treatment of the isomerization reactions

For a universe of 100 molecules the calculations were carried out as shown in the following example for 20% of total *Z* (*cis*) and 80% of total *E* (*trans*), where the symbol $C_p^n = n!/(n - p)!p!$ represents the combination of *n* elements *p* to *p*.

Species	Molar fraction
E-E	C_2^{80}/C_2^{100}
E-Z	$C_1^{80}C_1^{20}/C_2^{100}$
Z-Z	C_2^{20}/C_2^{100}

References

1 H. Rau, in *Photochromism Molecules and Systems*, eds. H. Dürr and H. Bouas-Laurent, Elsevier, Oxford, 1990, ch. 4.
2 V. Balzani and F. Scandola, *Supramolecular Photochemistry*, Ellis Horwood, Chichester, 1991, ch. 7.
3 (*a*) S. Shinkai, T. Nakaji, Y. Nishida and T. Ogawa, *J. Am. Chem. Soc.*, 1980, **102**, 5860; (*b*) S. Shinkai, T. Kounot, Y. Kusano and O. Manabe, *J. Chem. Soc.*, *Perkin Trans. 2*, 1982, 2741.
4 H. W. Losensky, H. Spelthann, A. Elhen, F. Vögtle and J. Bargon, *Angew Chem.*, *Int. Ed. Engl.*, 1988, **27**, 1189.
5 K. Ueno, H. Yoshimura, R. Saka and T. Osa, *J. Am. Chem. Soc.*, 1979, **101**, 2729.
6 K. Ueno, R. Saka and T. Osa, *Chem. Lett.*, 1979**,** 841.
7 S. Shinkai and O. Manabe, *Top. Curr. Chem.*, 1984, **121**, 67.
8 S. Shinkai, Y. Honda, Y. Kusano and O. Manabe, *J. Chem. Soc.*, *Chem. Commun.*, 1982, 848; S. Shinkai, Y. Honda, T. Minami, K. Ueda, O. Manabe and M. Tashiro, *Bull. Chem. Soc. Jpn.*, 1983, **56**, 1700; S. Shinkai, Y. Honda, K. Ueda and O. Manabe, *Israel. J. Chem.*, 1984, **24**, 302.
9 M. Shiga, M. Takagi and K. Ueno, *Chem. Lett.*, 1990, 1021.
10 S. Shinkai, T. Ogawa, T. Nakaji and O. Manabe, *J. Chem. Soc.*, *Chem. Commun.*, 1980, 375.
11 S. Shinkai, T. Nakaji, T. Ogawa, K. Shigematsu and O. Manabe, *J. Am. Chem. Soc.*, 1981, **103**, 111.
12 S. Shinkai, T. Ogawa, Y. Kusano, O. Manabe and K. Kikukaw, *J. Am. Chem. Soc.*, 1979, **101**, 1334.
13 A. Bianchi, M. Micheloni and P. Paoletti, *Coord. Chem. Rev.*, 1991, **110**, 17.
14 R. M. Izatt, K. Pawlak, J. S. Bradshaw and R. L. Bruening, *Chem. Rev.*, 1995, **33**, 2529.
15 *Supramolecular Chemistry of Anions*, eds. A. Bianchi, K. Bowman-James and E. Garcia-España, VCH-Wiley, New York, 1997.
16 P. Bortolus and S. Monti, *J. Phys. Chem.*, 1979, **83**, 648.
17 M. Ciampolini, P. Dapporto, M. Micheloni, N. Nardi, P. Paoletti and F. Zanobini, *J. Chem. Soc.*, *Dalton Trans.*, 1984, 1357.
18 C. G. Hatchard and C. A. Parker, *Proc. R. Soc. London*, *Ser. A*, 1956, **235**, 518.
19 A. Bianchi, L. Bologni, P. Dapporto, M. Micheloni and P. Paoletti, *Inorg. Chem.*, 1984, **23**, 1201.
20 G. Gran, *Analyst* (*London*), 1952, **77**, 661; F. J. Rossotti and H. Rossotti, *J. Chem. Educ.*, 1965, **42**, 375.
21 P. Gans, A. Sabatini and A. Vacca, *Talanta*, 1996, **43**, 1739.

Paper 7/04096B
Received 11*th June* 1997
Accepted 8*th October* 1997